

## Anomalous magnetic properties of the nano-size residual amorphous phase in nanocrystals

This article has been downloaded from IOPscience. Please scroll down to see the full text article.

1999 J. Phys.: Condens. Matter 11 L179

(<http://iopscience.iop.org/0953-8984/11/17/102>)

View [the table of contents for this issue](#), or go to the [journal homepage](#) for more

Download details:

IP Address: 171.66.16.214

The article was downloaded on 15/05/2010 at 07:20

Please note that [terms and conditions apply](#).

## LETTER TO THE EDITOR

**Anomalous magnetic properties of the nano-size residual amorphous phase in nanocrystals**

D Kaptás†, T Kemény†, J Balogh†, L Bujdosó†, L F Kiss†, T Pusztai† and I Vincze†‡

† Research Institute for Solid State Physics and Optics, H-1525 Budapest, POB 49, Hungary

‡ Department of General Physics, Eötvös University, Budapest, Hungary

Received 23 February 1999

**Abstract.** The composition dependence of the Curie temperature and the magnetic moment of the nano-size residual amorphous phase in partially crystallized  $\text{Fe}_{92-x}\text{Zr}_7\text{B}_x\text{Cu}_1$  ( $2 \leq x \leq 23$ ) amorphous alloys were determined by  $^{57}\text{Fe}$  Mössbauer spectroscopy. Both quantities show broad minima and for increasing relative Zr content (i.e. for decreasing B concentration) surpass the usual monotonic decrease observed for the bulk counterparts. The deviation does not scale with the characteristic size of the residual amorphous regions, which was found to be constant, ruling out explanations based on interphase exchange interaction. A magnetovolume origin of the observed anomalous composition dependence and the improved soft-magnetic characteristics of these nanocrystals is proposed.

The nanocrystalline (nc) Fe–M–B(Cu) alloys [1] (where M is an early transition metal such as Zr or Nb) and the earlier-discovered nc-Fe–Nb–Si–B(Cu) alloys [2] (i.e. FINEMET) show superior soft-magnetic properties (high initial permeability together with a substantial saturation magnetization). They are prepared by partial crystallization of amorphous ribbons which produces nano-size crystalline bcc precipitates in a residual amorphous matrix. The explanation of the good soft-magnetic properties is of both fundamental and technical interest and at present it is a controversial issue. It is generally acknowledged that the reduction of the effective magnetocrystalline anisotropy on forming ultrafine grains plays a decisive role. Since the observation that in nc-Fe–Nb–Si–B(Cu) alloys the good soft-magnetic properties show a fast deterioration above the Curie temperature,  $T_c$ , of the ferromagnetic residual amorphous phase, an important role of the connecting tissue in the coupling of the ferromagnetic bcc grains is implied [2]. However, in contrast to this behaviour, for nc-Fe–Zr–B–Cu alloys the coercivity and permeability exhibits no temperature anomaly at the Curie temperature of the residual amorphous phase [3, 6]. Resolution of the apparent controversy was attempted [3, 7] by introducing the idea of the penetration of the bcc grains' ferromagnetic exchange interaction into the intergranular amorphous matrix resulting in an indirect exchange coupling between the adjacent ferromagnetic grains. This hypothesis would involve two consequences: an enhancement and a considerable smearing out of the Curie temperature of the residual amorphous phase. Indeed, magnetic measurements reported in [8] indicated an increase of the Curie temperature of the intergranular amorphous regions in nanocrystalline alloys of the order of 100 K. On the other hand,  $^{57}\text{Fe}$  Mössbauer measurements indicated [9, 10] neither appreciable smearing out of the Curie temperature of the amorphous residual phase nor significant increase in its Curie temperature, further obscuring the origin of the good soft-magnetic properties of these alloys. The relative importance of the intergranular exchange

and the dipolar interactions for the magnetic behaviour of granular magnetic alloys is an open and fundamental question [11]. Comparison of the magnetic behaviour of the nano-size residual amorphous phase and that of the bulk amorphous counterparts could substantially contribute to the understanding of the respective roles of these interactions. Earlier reports focused on the technically important compositions and no systematic concentration dependence studies were published for which the concept of exchange penetration could be critically tested by establishing the characteristic size relations of the different phases. In this letter a systematic temperature-dependent Mössbauer study of the residual amorphous matrix for a wide composition range of nc-Fe-Zr-B(Cu) alloys, carried out to elucidate the role of the interactions, is reported.

The nanocrystalline  $\text{Fe}_{92-x}\text{Zr}_7\text{B}_x\text{Cu}_1$  ( $2 \leq x \leq 23$ ) samples were produced from amorphous ribbons (melt spun in a protective atmosphere). DSC results have confirmed [6] that crystallization occurs in two widely separated transformation stages, with heat evolution practically absent between the two stages. The nc samples were produced by heat treatment up to the appropriate temperature of the end of the first crystallization stage (typically at around 900 K). The hyperfine parameters and the grain sizes of the samples quenched from different temperatures over a 50 K range at the end of this stage were found to be identical within the experimental error. The nanocrystalline state was verified and the grain sizes of the bcc granules were determined by x-ray diffraction with a Philips Xpert diffractometer using Cu  $K\alpha$  radiation and Bragg-Brentano geometry. For  $x = 6$ , synchrotron x-ray powder diffraction experiments were also performed. At this composition the grain size was also determined [6] by cross sectional transmission electron microscopy (TEM), and found to be in reasonable agreement with the x-ray result.  $^{57}\text{Fe}$  Mössbauer spectroscopy measurements were performed between 4.2 K and 900 K.

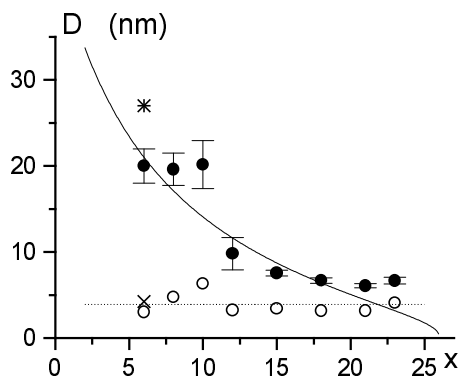


**Figure 1.** The composition dependence of the bcc grain size,  $D$  (full circles), measured by means of x-ray diffraction and the calculated characteristic size of the residual amorphous phase,  $d$  (empty circles). The calculated full curve shows the composition trend of  $D$  as explained in the text; the broken line corresponds to the average value of  $d$ . Similar data for nc- $\text{Fe}_{87}\text{Zr}_6\text{B}_6\text{Cu}_1$  are also shown ( $D$ : star;  $d$ : cross) [14].

The average grain size of the nanocrystals,  $D$ , has been determined from the additional line broadening of the bcc lines (i.e., that beyond the instrumental resolution, determined using a standard Si sample). The Rietveld full-profile matching technique was applied using the program FULLPROF. The results are shown in figure 1. The determination is straightforward when the corrections to the line broadening are small, i.e. when the average grain size is below about 15 nm. At larger grain sizes the proper deconvolution of the size and strain broadening involves [12] more sophisticated methods. Texture effects can further disturb the particle

size evaluation and prevented reliable determination of the grain sizes for  $x = 2$  and 4. The inherent limitations of the grain size determination are also evident, as the results obtained by different methods may deviate significantly. Small-angle x-ray scattering for example yielded grain size values which are a factor of 2 smaller than those obtained from the x-ray diffraction broadening due to the different averaging [13].

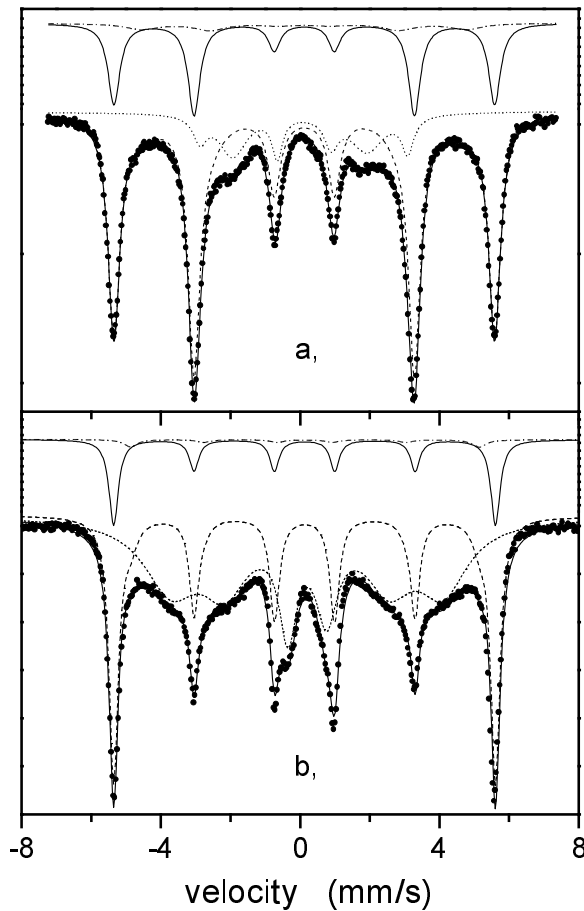


**Figure 2.** Mössbauer spectra of  $\text{nc-Fe}_{90}\text{Zr}_7\text{B}_2\text{Cu}_1$  (a) and  $\text{nc-Fe}_{69}\text{Zr}_7\text{B}_{23}\text{Cu}_1$  (b) taken at 4.2 K. The full curve is the fitted curve; the bcc nanocrystalline component (broken curve) and the residual amorphous part (dotted curve) are also marked. The bcc component is made up of two contributions as shown in the upper part of the figure: the main lines (continuous curve) and the satellite, i.e., the shoulder lines (dash-dot curve), are shown.

In figure 2 a typical Mössbauer spectrum, that of  $\text{nc-Fe}_{90}\text{Zr}_7\text{B}_2\text{Cu}_1$  measured at 4.2 K, is shown. It has two characteristic features: a narrow sextet with an asymmetric shoulder which can be attributed to the bcc granules and a broad magnetic component belonging to the residual amorphous phase. The Mössbauer parameters (isomer shift,  $IS_m$ , and hyperfine field,  $B_m$ ) of the stronger component of the asymmetric sextet, which will be referred to as the main line, are similar to those of pure bcc Fe at low temperatures.  $B_m$ , however, decreases with increasing temperature definitely faster than the hyperfine field of pure bcc Fe, indicating a lower Curie temperature than that of  $\alpha$ -Fe. The main line has a shoulder on the low-field side which is quite broad; its hyperfine field is  $B_s$ . This shoulder is often attributed [14, 15]

to an interfacial phase. However,  $B_s$  closely follows the temperature dependence of  $B_m$  over a broad temperature range [10, 16], supporting the assertion that the nanocrystalline Fe-based bcc phase contains a few per cent of dissolved Zr and B (less than about 4 at.%). Thus  $B_m$  is the hyperfine field of Fe atoms with no Zr or B nearest and next-nearest neighbours and  $B_s$  is the average hyperfine field of Fe atoms with at least one impurity neighbour in the first two coordination shells. The relative amounts of Fe in the main and in the shoulder components are  $n_m$  and  $n_s$ , respectively.

The total relative number of Fe atoms in the bcc phase,  $n_{\text{bcc}} = n_m + n_s$ , shown in figure 3(a), allows an estimation of the iron content of the residual amorphous phase. The small

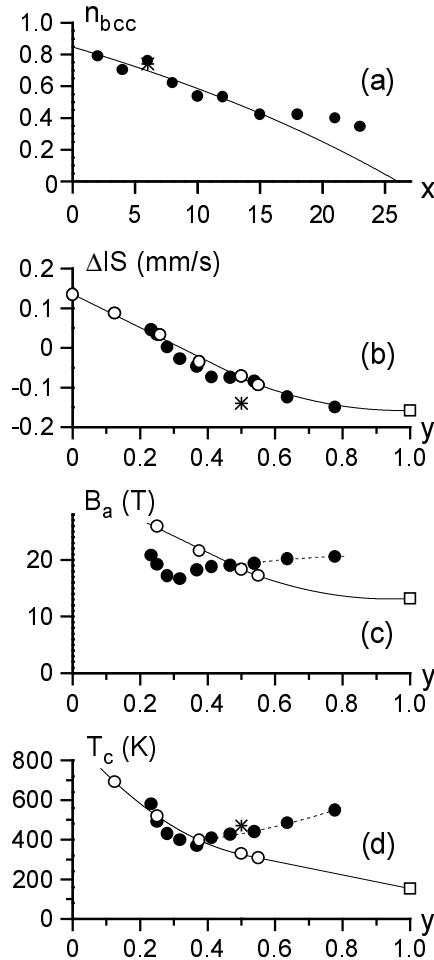


**Figure 3.** The composition dependence of the relative number of Fe atoms in the bcc granules,  $n_{\text{bcc}}$  (a), the isomer shift with respect to that of  $\alpha$ -Fe,  $\Delta\text{IS}$  (b), the average Fe hyperfine field,  $B_a$  (c) and the Curie temperature (d) in the residual amorphous phase (full circles). The calculated continuous curve in (a) corresponds to the relative amount of iron content in the case of  $\alpha$ -Fe precipitations when the Fe content of the residual phase is 66.7 at.%. The data for bulk amorphous  $\text{Fe}_2(\text{B}_{1-y}\text{Zr}_y)$  are taken from [18] (empty circles) and [19] (empty squares) ( $y = 7/(7+x)$ ). Stars show similar data for nc- $\text{Fe}_{37}\text{Zr}_6\text{B}_6\text{Cu}_1$  (the assignment of  $n_{\text{bcc}}$  applied here is used) [14]. The broken and the continuous curves in panels (b), (c) and (d) are guides to the eyes showing the trends in the nano-size phase and in the bulk phase, respectively.

amount of Cu, whose main role is triggering the nanocrystal formation by precipitating in a separate fcc phase [17], and the Zr/B content of the bcc phase are entirely neglected in plotting the calculated curve of figure 3(a), which corresponds to 66.7 at.% Fe content of the residual amorphous phase. The measured values follow the calculated curve well; deviation is only observed at large Zr + B content. If we assume that the starting Zr-to-B ratio of the precursor amorphous phase remains unchanged during the nanocrystallization, the composition of the residual amorphous phase is approximated as  $\text{Fe}_2(\text{B}_{1-y}\text{Zr}_y)$ , where  $y = 7/(7+x)$ . A relevant parameter for the composition of the residual amorphous phase is its isomer shift, since it is dominantly determined by the numbers of Zr and B nearest neighbours of iron. In bulk amorphous  $\text{Fe}_2(\text{B}_{1-y}\text{Zr}_y)$  alloys a significant isomer shift change exceeding  $0.2 \text{ mm s}^{-1}$  is observed [18] and this is reproduced in figure 3(b). The measured isomer shift of the residual amorphous phase,  $\Delta\text{IS}$ , follows this trend well, supporting the supposed similarity of the compositions.

The residual amorphous phase is characterized by a hyperfine-field distribution; its average hyperfine field is  $B_a$ . Figure 3(c) compares the composition dependence of  $B_a$  to that of the bulk amorphous  $\text{Fe}_2(\text{B}_{1-y}\text{Zr}_y)$  alloys. The hyperfine-field distribution of the residual amorphous phase has a low-field tail not observed [18] for the bulk alloys, which is a sign of concentration fluctuations and gradients developing in the process of the precipitation of the bcc phase. This feature of the hyperfine-field distributions explains the reduction of the average  $B_a$ -values of the residual amorphous phase. Despite this behaviour,  $B_a$  surpasses the values for the bulk alloys when  $y > 0.5$ .

The atomic crystalline fraction of Fe in the bcc granules,  $p$ , is calculated from the value of  $n_{\text{bcc}}$  on the above-mentioned assumptions. The characteristic size,  $d$ , of the residual amorphous tissue can be estimated as [8]  $d = D(p^{-1/3} - 1)$ , where  $p$  is used as a volume fraction, neglecting density differences. The  $d$ -values deduced are shown in figure 1; they are independent of the composition, with an average value of  $3.9 \pm 0.4 \text{ nm}$ . This agrees well with direct TEM measurements, where the presence of intergranular amorphous layers with size below 5 nm is reported [20]. In this way, the observed decrease of the bcc grain size with increasing amount of alloying elements in the precursor amorphous phase can be explained by the formation of the amorphous  $\text{Fe}_2(\text{B}_{1-y}\text{Zr}_y)$  layers which serve as a diffusion barrier due to their relative stability. Small bcc grain sizes are expected when the composition of the starting amorphous alloy is near to 66.7 at.% Fe content. The grain size is expected to grow with increasing Fe content of the precursor (i.e. with decreasing Zr + B content) until it reaches the specified barrier composition. The calculated curve for  $D$  in figure 1 is based on the assumptions that the residual amorphous phase has 66.7 at.% Fe content and its characteristic size,  $d_0$ , is independent of the composition, i.e.  $D = d_0\{[100/(78 - 3x)]^{1/3} - 1\}$ . The average value of  $d_0 = 3.9 \text{ nm}$  was chosen, leaving no free parameters for the calculated curve. The overall agreement with the measured values is acceptable; significant deviation is observed at high impurity composition, explained by the neglected impurity content in the bcc granules, as for  $n_{\text{bcc}}$ .

The Curie point of the residual amorphous phase,  $T_c$ , was determined from the standard plot of  $B_a^3$  versus  $T$ , which is analogous to the often-used magnetic method [2, 8]. The transition is reasonably sharp; the spread in  $T_c$  is partly due to the concentration fluctuations and partly due to the stray magnetic field (1–2 T) of the adjacent ferromagnetic granules [9, 10].

The composition dependence of the Curie point of the residual amorphous phase in  $\text{nc-Fe}_{92-x}\text{Zr}_7\text{B}_x\text{Cu}_1$  is compared in figure 3(d) with that [18] of the bulk  $\text{Fe}_2(\text{B}_{1-y}\text{Zr}_y)$  amorphous alloys, where  $y = 7/(7+x)$ . The bulk  $T_c$ -values decrease monotonically for increasing  $y$  up to  $y = 0.55$ , which was the limiting composition for sample preparation by melt quenching. They extrapolate smoothly to the value for amorphous  $\text{Fe}_2\text{Zr}$  interpolated [19] for sputtered samples.

In general, this is the expected behaviour of  $T_c$  for the simple replacement of nonmagnetic elements, and it is indeed observed [21,22] e.g. for the crystalline  $\text{Fe}_2(\text{Zr}_{1-y}\text{Nb}_y)$  alloys and for the amorphous  $\text{Fe}_{80}\text{B}_{20-x}\text{Zr}_x$  alloys. The Curie temperature of the residual amorphous phase follows the decreasing trend of the bulk alloys well for  $y$  up to about  $y \approx 0.4$ , then progressively exceeds it, giving a broad minimum. Obviously this unexpected composition behaviour of  $T_c$  for the nano-size residual amorphous phase cannot be explained by a model based on the exchange-field penetration from the bcc crystallites [7, 8, 14] since the characteristic size of the residual amorphous phase was found to be independent of the composition. An earlier-reported [14] quantitative agreement of the increase in  $T_c$  for nc- $\text{Fe}_{87}\text{Zr}_6\text{B}_6\text{Cu}_1$  with this model is a consequence of a linear extrapolation of the  $T_c$ -values for bulk amorphous  $\text{Fe}_{100-2x}\text{Zr}_x\text{B}_x$  alloys which is not supported by the experiments [18, 22].

On the other hand, the unusual increase of  $T_c$  for the residual amorphous phase with increasing Zr content seems to correlate well with the similarly surprising increase in the average iron hyperfine field, i.e. in the average iron magnetic moment of this phase (figure 3(c)). It is well known [23] that the magnetic properties of amorphous Fe–Zr alloys show strong magnetovolume effects: both the Curie temperatures and the iron magnetic moments increase with increasing iron atomic volume, which is achieved by alloying small-volume components like H or B. The explanation of the anomalously large  $T_c$  and Fe magnetic moments for the residual amorphous phase necessitates even larger Fe volume expansion which may have two possible origins. The strong attractive interaction between the Zr and B components observed in bulk  $\text{Fe}_2(\text{B}_{1-y}\text{Zr}_y)$  glasses [18] may increase the atomic volume of the Fe atoms in the residual amorphous phase formed under quasi-equilibrium conditions as compared to that in the bulk amorphous alloys prepared by rapid quenching. The larger density (reduced volume) of the precipitated bcc granules in the nanocrystals results in a tensile stress which may also cause an excess volume for the Fe atoms in the connecting tissue. For the range of grain sizes investigated, this tensile stress (and thus the excess Fe atomic volume in the residual amorphous phase) should increase with the amount of precipitated bcc phase.

The average hyperfine field (i.e. Fe magnetic moment) and the Curie point of the residual amorphous phase gradually deviate with decreasing B content from the usual decreasing trend of the bulk counterpart. The optimal composition for soft-magnetic characteristics [6] (nc- $\text{Fe}_{90}\text{Zr}_7\text{B}_2\text{Cu}_1$ ) coincides with the composition for which the largest anomaly of the fundamental magnetic properties of the residual amorphous phase is observed for nc- $\text{Fe}_{92-x}\text{Zr}_7\text{B}_x\text{Cu}_1$  alloys. It is implied that the tensile stress produced by the precipitated bcc grains might be a common explanation through magnetovolume effects. This volume effect seems to be analogous on a nanometre scale with the well-known influence of Si in the conventional Fe–Si soft-magnetic materials, for which the decreased magnetocrystalline anisotropy is also connected with the reduction of the bcc cell volume.

We are grateful to Dr Gy Faigel for useful discussions of the grain size determination. This work was supported by the Hungarian Research Fund (OTKA T022413 and T020962).

## References

- [1] Suzuki K, Makino A, Inoue A and Masumoto T 1991 *J. Appl. Phys.* **70** 6232
- [2] Herzer G 1993 *Nanomagnetism* ed A Hernando (Dordrecht: Kluwer–Academic) p 111  
Herzer G 1995 *Scr. Metall.* **33** 1741
- [3] Hernando A and Kulik T 1994 *Phys. Rev. B* **49** 7064
- [4] Gómez-Polo C, Holzer D, Multigner M, Navarro E, Agudo P, Hernando A, Vázquez M, Sassik H and Grössinger R 1996 *Phys. Rev. B* **53** 3392
- [5] Suzuki K and Cadogan J M 1998 *Phys. Rev. B* **58** 2730

- [6] Kemény T, Varga I K, Kiss L F, Balogh J, Lovas A, Tóth L and Vincze I 1997 *Mater. Sci. Eng. Suppl.* A 201
- [7] Navarro I, Ortuno M and Hernando A 1996 *Phys. Rev. B* **53** 11 656
- [8] Hernando A, Navarro I and Gorria P 1995 *Phys. Rev. B* **51** 3281  
Hernando A, Navarro I, Prados C, Garcia D, Vázquez M and Alonso J 1996 *Phys. Rev. B* **53** 8223
- [9] Kemény T, Balogh J, Farkas I, Kaptás D, Kiss L F, Pusztai T, Tóth L and Vincze I 1998 *J. Phys.: Condens. Matter* **10** L221
- [10] Kemény T, Kaptás D, Balogh J, Kiss L F, Pusztai T and Vincze I 1999 *J. Phys.: Condens. Matter* **11** 2841
- [11] Ferreira M S, d'Albuquerque e Castro J, Muniz R B and Lopes L C 1998 *Phys. Rev. B* **58** 8198  
El-Hilo M, Chantrell R W and O'Grady K 1998 *J. Appl. Phys.* **84** 5114
- [12] Ungár T and Borbély S 1996 *Appl. Phys. Lett.* **69** 3173
- [13] Kopcewicz M, Grabias A and Williamson D L 1997 *J. Appl. Phys.* **82** 1747
- [14] Garitaonandia J S, Schmool D S and Barandiarán J M 1998 *Phys. Rev. B* **58** 12 147
- [15] Miglierini M and Greneche J M 1997 *J. Phys.: Condens. Matter* **9** 2303  
Miglierini M and Greneche J M 1997 *J. Phys.: Condens. Matter* **9** 2321
- [16] Vincze I, Kemény T, Kaptás D, Kiss L F and Balogh J 1998 *Hyperfine Interact.* **113** 123
- [17] Ayers J D, Harris V G, Sprague J A, Elam W T and Jones H N 1998 *Acta Metall. Mater.* **46** 1861  
Hono K and Sakurai T 1997 *Sci. Rep. RITU A* **44** 223
- [18] Kaptás D, Kemény T, Balogh J, Bujdosó L, Kiss L F, Pusztai T and Vincze I 1999 *J. Phys.: Condens. Matter* **11** L65
- [19] Unruh K M and Chien C L 1984 *Phys. Rev. B* **30** 4968
- [20] Makino A, Inoue A and Masumoto T 1995 *Mater. Trans. JIM* **36** 924
- [21] Kanematsu K 1969 *J. Phys. Soc. Japan* **27** 849
- [22] Ohnuma S, Nose M, Shirakawa K and Masumoto T 1981 *Sci. Rep. RITU A* **29** 254
- [23] Ryan D H, Coey J M D, Batalla E, Altounian Z and Ström-Olsen J O 1987 *Phys. Rev. B* **35** 8630  
Shen Bao-gen, Xu Rufeng, Zhao Jian-gao and Zhan Wen-shan 1991 *Phys. Rev. B* **43** 11 005